International Journal For Technological Research In Engineering
Volume 3, Issue 9, May-2016 *ISSN (Online): 2347 - 4718*

CHARACTERIZATION & FABRICATION OF $PR_{0.7}BA_{0.3-X}K_XMNO_3$ ($0 \leq X \leq 0.1$)

Dr. Kirti Vishwakarma[1], Er. K. C. Priydarshi[2]
Department of Nanotechnology Gyanganga College of Technology Jabalpur

Abstract: Over the year, the perovskite manganites R1-xAxMnO3 (R= rare earth and A = alkaline earth) have become the center juncture in advance materials science owing to the promising applications of these materials for magnetic sensors, spintronics and bolometric devices etc [1-5]. These materials offer a high degree of chemical flexibility leading to complex interplay between structural, electronic and magnetic properties. By the partially substitution divalent/monovalent ions at the rare earth site, the resistivity profile exhibits a metal-insulator transition phenomenon at temperature (Tp) and these samples show paramagnetic insulator behavior above Tp and ferromagnetic metal behavior below Tp [6]. The double exchange (DE) mechanism used to explain the nature of attraction, metallic behavior of the material below the insulator – metal transition temperature (Tp) [7]. The resulting strong interaction among spin, charge, lattice/orbital degrees of freedom depends on which interactions dominate. It can be tuned by dopants, the application of external magnetic field, pressure, electric field, radiation etc [8-10]. However, several studies have shown that Jahn-Teller (JT) distortion and grain boundary (GB) effects also a imperative function to comprehend the physics lying in these CMR materials [7].

During last decade the influence of rare earth site substation by a divalent and trivalent element and Mn site substitution have been extensively studied [11-13]. Although very few reports are on monovalent alkali metal ion doped system. The monovalent substitution directly affect the ratio of Mn3+ and Mn4+ ions as compared to divalent which ultimately affects the DE mechanism and hence the magento transport properties in a way different form that of the divalent cation substituted manganites [14]. Further, the crystal structure may be modified depending on the radius of monovalent ions [15]. Lakshmi et al. [16] successfully reported that the influence of silver doping on the electrical and magnetic behavior of La0.7Ca0.3MnO3 (LCMO) manganites. Earlier the of Ag+ cation on La0.7Sr0.3MnO3 (LSMO) structural and magneto transport properties with no improvement in MR values have been reported [17]. However, Yadav et al. [18] observed the improvement in magento resistance (MR) and temperature coefficient of resistance (TCR) with monovalent Ag+ substitution on LSMO compounds. On the other hand, the sintering temperature promotes grain growth, improves connectivity between the grains also plays a major role in deciding the electronic and magnetic properties in polycrystalline CMR materials. The grain boundaries can be altered with sintering temperature which influences electrical and magnetic properties [19-21]. Chang et al. [21] have paid much attention to investigate the effect of sintering temperature on the electrical and wide range magneto resistance which shows improvement in magneto resistance, suppression of resistivity at larger instant. Similarly Yadav et al. [15] obtained the large enhancement in magneto resistance as function of sintering temperature in La0.7Ca0.3-xAgxMnO3 system.

In the present work, we have synthesized Pr0.7Ba0.3-xKxMnO3 ($0 \leq x \leq 0.1$) compounds by sol gel technique to understand the influence of monovelent K cation doping on magneto-resistance (MR) behavior. We observed very high wide range magneto-resistance on doping which from the application point of view can be used to tune the sensing mechanism in bolometric sensors.

The work is carried out with following objectives in mind as under.

- Single Phase synthesis of pure Pr0.7Ba0.3-xKxMnO3 ($0 \leq x \leq 0.1$).
- Structural analysis using X-ray diffraction and POWDER X programme.
- Study of low temperature resistivity of Pr0.7Ba0.3-xKxMnO3 ($0 \leq x \leq 0.1$).
- Analysis of data and understanding of the underlying physical phenomena.

I. SYNTHESIS AND CHARACTERIZATION TECHNIQUE

Sol-Gel Techniques:

Sol-gel is a wet-chemical-based self-assembly process for nonmaterial formation. The sol-gel process involves the evolution of networks through the formation of a colloidal suspension (sol) and gelation of the sol to form a network in a continuous liquid phase(gel). “Sol” describes the dispersion of colloids, i.e., particles in the range of 1 - 100 nm diameters in liquids[1]. If the viscosity of the “sol” is made to increase sufficiently e.g., by partial loss of the liquid phase, it becomes a rigid “gel”. Sol-gel technique can be used for several purposes including the formation of fine powders, homogeneous thin and thick films, fibers, homogeneous bulk material, porous solids and powders. There has been considerable development in sol-gel techniques resulting from applications dependent on organic solvents, as even nano-scale particles can be prepared. An example of the use of organic solvents is the use of metal alk-oxide precursor method.

Thegel process generally involves the use of metalalkoxides, which undergo hydrolysis a nd condensation polymerization reactions to give gels [2]. A catalyst is used to start reaction and control pH. Sol-gel formation occurs in four stages.

- Hydrolysis
- Condensation
- Growth of particles
- Agglomeration of particles

Hydrolysis: During hydrolysis, addition of water results in the replacement of [OR] group with [OH-] group. Hydrolysis occurs by attack of oxygen on silicon atoms in silica gel. Hydrolysis can be accelerated by adding a catalyst such as HCl and NH3. Hydrolysis continues until all alkoxy groups are replaced by hydroxyl groups. Subsequent condensation involving silanol group (Si-OH) produced siloxane bonds (Si-O-Si) and alcohol and water. Hydrolysis occurs by attack of oxygen contained in the water on the silicon atom.

Condensation: Polymerization to form siloxane bond occurs by either a water producing or alcohol producing condensation reaction. The end result of condensation products is the formation of monomer, dimer, cyclic tetramer, and high order rings. The rate of hydrolysis is affected by pH, reagent concentration and H2O/Si molar ratio (in case of silica gels). Also ageing and drying are important. By control of these factors, it is possible to vary the structure and properties of sol-gel derived inorganic networks.

Growth and Agglomeration: As the number of siloxane bonds increase, the molecules aggregate in the solution, where they form a network, a gel is formed upon drying. The water and alcohol are driven off and the network shrinks. At values of pH of greater then 7, and H2O/Si value ranging from 7 to 5[3]. Spherical nano-particles are formed. Polymerization to form siloxane bonds by either an alcohol producing or water producing condensate occurs.

Above pH of 7, Silica is more soluble and silica particles grow in size. Growth stops when the difference in solubility between the smallest and largest particles becomes indistinguishable. Larger particles are formed at higher temperatures. Laser vaporization technique has offered several advantages over other heating techniques. A high energy pulsed laser with an intensity flux of 106 - 107 W/cm2is forced on target material. The plasma causes high vaporization and high temperature (10,000°C). Typical yields are 1014-1015 atoms from the surface area of 0.01 cm2 in a 10-8 s pulse. Thus a high density of vapor is produced in a very short time (10-8 s), which is useful for direct deposition of particles.

Electro-deposition: Nano-structured materials can also be produced by electro-deposition. These films are mechanically strong, uniform and strong. Substantial progress has been made in nano-structured coatings applied either by DVD or CVD. Many other non-conventional processes such as hypersonic plasma particle deposition (HPPD) have been used to synthesize and deposit nano-particles. It has been shown that certain properties of nano-structured deposits such as hardness, wear resistance and electrical resistivity are strongly affected by grain size. A combination of increased hardness and wear resistance results in a superior coating performance.

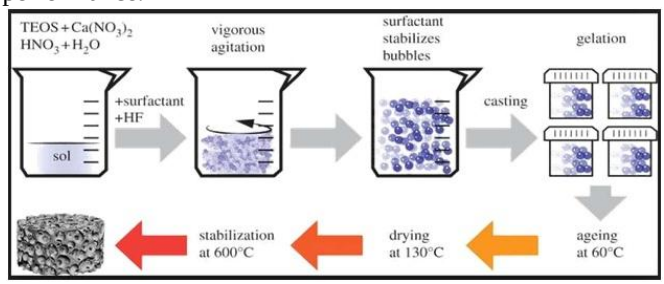

Figure : Sol-gel synthesis technique. (Ref.2)

Sol-gel Chemistry:

Chemistry involved in the sol-gel process is very important for the proper fabrication of the required material. Initial conditions such as pH of sol, cation concentration, temperature, time etc. control the sol-gel chemistry. The chemical reaction taking place behind the various steps involved in the sol-gel process. The probable chemical reactions for various steps in sol-gel process are discuss below:

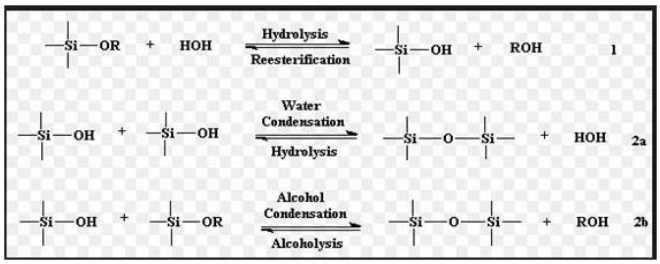

Figure: Sol-gel Chemistry. (Ref.2)

There are several advantages of sol-gel technique, such as

- As the process is based on chemical reactions in liquid phase, it is very simple technique.
- It is cost-effective, as very simple accessories are needed for the chemical reaction and deposition procedure.
- Due to chemical involved in the process, a large range of material can be deposited by this technique.
- As the deposition is done in liquid phase, the process is versatile enough to procedure a large form of materials starting from aerogel, xerogel, ceramic materials, nano-powders, nano-structured thin film etc.
- Control over the doping level is also easier in this process.
- Possibility of high purity of starting material can be achieved.

Characterization Technique:

After the preparation of the sample , the most important step is to characterize the prepared sample by using different methods to explore the exact information of the material.

Here we have used the following characterization techniques

X-ray Diffraction (XRD):
XRD is one of the most important experimental techniques to address all the issues related to crystal structure of solids, including lattice constants and geometry, identification of unknown materials, orientation of single crystal, defects, stresses etc. A careful XRD analysis gives a clear picture about the different phases present in the specimen.
The role of X-rays diffraction experiment is based on the electromagnetic properties of this form of radiation. Electromagnetic radiation such as visible light and x-ray can sometimes behave as if the radiation were a beam of particles, while at other times it behaves as if the radiation were a wave. If the energy emitted in the form of photons has a wavelength 10-6 to 10-10cm. Then the energy is referred to as X-rays. Electromagnetic radiation can be regarded as a wave moving at the speed of light (3x10 10cm/s in a vacuum) and having associated with it a wavelength, and a frequency.
The colors of the visible range of the spectrum are violet(V), indigo(I), blue(B), green(G), yellow(Y), orange(O), and red(R).

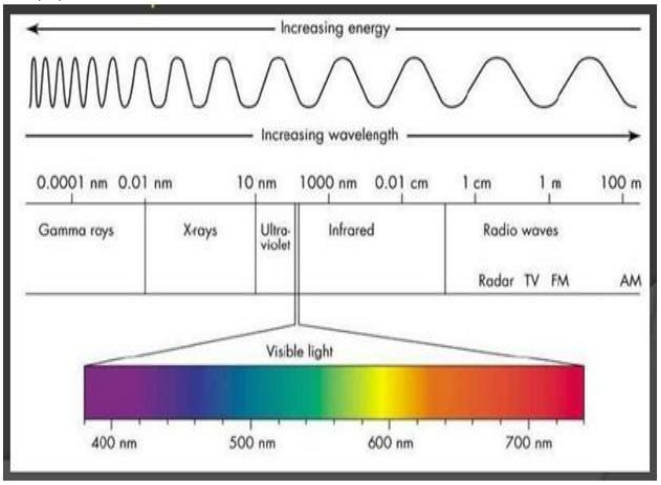

Figure 2.3: Electromagnetic Spectrum. (Ref.3)

X-rays are electromagnetic radiations with typical photon energies in the range of 100ev-1000ev. For diffraction applications, only short wavelength. Since the wavelength of x-ray is comparable to the size and inters atomic distances of the atom, they are ideally suited for probing the structural arrangement of atoms and hence provide detailed information about the various structure. X-ray primarily interacts with electron in the atoms when x-ray photons collide with electrons some photons from the incident beam will be deflected away from the direction where they originally travel. These are the x-ray that we measure in the diffracted experiment, as the scattered x-ray carry information about the atom distribution in materials . Diffracted x-ray from different atoms can interference with each other and resultant intensity distribution is strongly modulated by this interaction. If the atoms are arranged in a periodic array, the diffracted waves will consists of sharp interference maxima with the same symmetry as in the distribution of atoms.

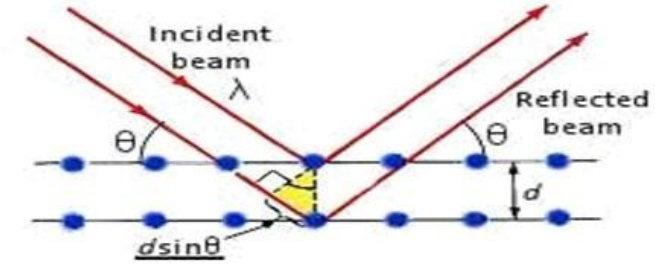

Figure: Reflections of X-ray from lattice planes in a crystal.

In XRD , a collimated beam of x-rays, with a wavelength typically ranging from 0.7 to 2Å, is incident on a specimen and is diffracted by the crystalline phases in the specimen according to Bragg‟s law:

$N\lambda = 2d \sin\theta$

where d is the spacing between atomic planes in the crystalline phase and λ is the X-ray wavelength, N is the number of planes. The intensity of the diffracted X-ray is measured as a function of the diffraction angle 2θ and the specimen‟s orientation. This diffraction pattern is used to identify the specimen‟s crystalline phases and to measure its structural properties.

Diffraction peak positions are accurately measured with XRD, which makes it the best method for characterizing homogenous and inhomogeneous strains.

If there is no inhomogeneous strain, the crystalline size D can be estimated from the peak width with Scherrer‟s formula:

$D = (K\lambda) / B \cos\theta_B$

Where λ is the X-ray wavelength, B is the full width of height maximum of a diffraction peak, θ_B is the diffraction angle and K is the Scherrer‟s constant. Typical intensities for electron diffraction are ~ 10^8 times larger than for XRD. X-ray diffraction only provides the collective information of the particle size and usually requires a sizable amount of powder. This technique is very useful in characterizing nano-particles.

Figure: X-ray Diffraction Equipment.

Powder XRD is perhaps the most widely used XRD technique for characterizing polycrystalline materials. The term „powdered" really means that the crystalline domains are randomly oriented in the sample and is usually in the powder form, consisting of fine grains of single crystalline material to be studied. Then XRD pattern is recorded, it shows concentric rings of scattering of the scattering peaks corresponding to the various d-spacing in the crystal lattice. The position and the intensities of the peaks are used for identifying the underlying structure of the material. The powder method is used to determine the values of the lattice parameters accurately. Lattice parameters are the magnitude of the unit vector a, b and c which define the unit cell for the crystal. The structural studies for the sample for under present studied are perform by XRD.

When electromagnetic radiations overlap in space simultaneously, either constructive or destructive interference occurs. Constructive interference occurs when the waves are moving in the step with one another. The waves reinforce one another and are said to be in phase, with one wave at maximum amplitude while the other is at minimum amplitude interference occur among the wave scattering by the atoms when crystalline solids are exposed to X-rays. The atom in the crystal scatters the incoming radiation, resulting in the diffraction patterns. Destructive interference occurs when the waves are out of phase with one another.

R-T Measurement:
There are different methods for resistivity measurement like this probe, collinear four probe, square four probe, electrometers and five probe method. A complete R-T measurement set up consists of constant current source, a sensitive voltmeter, a cryostat and a temperature controller. We used square four probe method for electrical resistivity measurement in which a square shaped sample is used. Four good indium contents are made in which current and voltage is applied diagonally. The sample is mounted in closed cycled refrigerator which can go down to I 0K.
The sample under present studies is characterized for the electrical transport studies by the experimental technique described below:
Resistivity and magnetic susceptibility both are used for measuring the critical/transition temperature. However, since the critical temperature TC (H, l) depends on both applied field on current, Tc (0.0) can only be measured approximately at low field and at low current. At temperatures below TC the resistivity of superconductor becomes very small, values less than 10-23Ω cm have been measured in conventional low temperature superconductor by persistent current with increasing currents, especially in the high temperature. Superconductor the resistivity is complicated by significant resistive flux flow, especially as T >= Tc. The measurement of zero resistance therefore requires definition concerning what exactly is to be measured. Zero resistance is sometimes defined as a resistivity less than that of Cu at the same temperature, (~ 10-8 Ω cm), sometimes the zero resistance of a material is defined by some ratio of its resistance to its resistance at a temperature. Just greater than T, i.e. above the one set of superconductivity. This definition is given to match the sensitivity of the measuring apparatus. The measurement of true residual resistance of temperatures $0 < T < Tc$ is generally beyond the sensitivity of the four-probe techniques, but magnetic signal can be used to further characterize material at these temperatures[4]. The dc resistivity of a sample is measure by the voltage drop across a specimen when a current of known magnitude which is typically around 1mA.

Figure: R-T Measurement set-up.

The terminals used for measuring voltage pass little current when connected to a high impedance voltmeter. These terminals are distinct from those used for passing the main part of the current through the specimen, where voltage drops in both heads and contacts are significant. The figure shows a schematic diagram of four probes connected to a specimen whose temperature is measured b a temperature specimen [5]. The resistivity measured is not necessarily a bulk property.

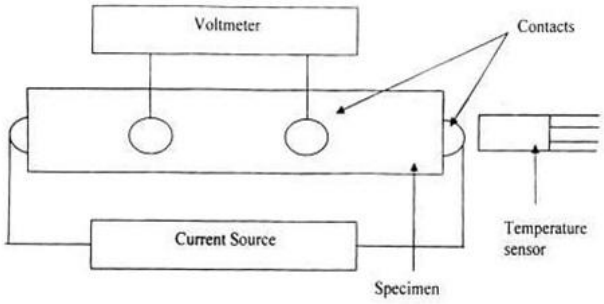

Figure 2.7: Schematic diagram of four probes.

A similar four probe apparatus can be used for elementary measurement of T_C, defined according to the sensitivity of the apparatus or to a selected criterion. In bulk material, the specimen, e.g. $LaCaMnO_3$ mounted on a thermally compatible, insulating substrate for mechanical strength. The contacts must have low resistance to reduce heating effect. The heating effects of the high currents at contacts and neck is further reduced by use of a pulsed current source starting with the low current, this is increased until the voltage drop, observed with a rapid voltage monitor. Such as oscilloscope,

reaches a defined level corresponding to T_C. a.c, resistivity can be measured by a similar four probe arrangement but using an a.c. current source and neck in amplifier for voltage measurement. Signal noise is reduced by the use of a preamplifier close to the specimen. In the present work a low temperature R-T setup as shown in figure is used.

XRD:

The X-ray diffraction patterns of $Pr_{0.7}Ba_{0.3-x}K_xMnO_3$ ($0 \leq x \leq 0.1$) are shown in Fig. 1. There are no new peaks which suggest that all the samples are single phase without any detectable impurity or any additional phase.

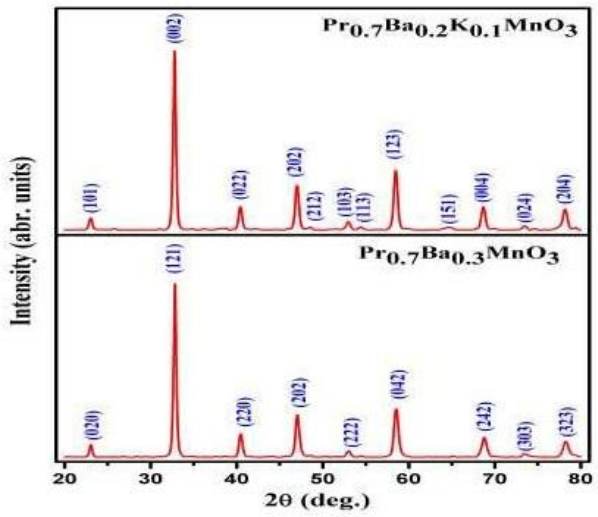

Fig: X-Ray Diffraction of $Pr_{0.7}Ba_{0.3-x}K_xMnO_3$ ($0 \leq x \leq 0.1$).

The lattice parameters and all relevant parameters of interest are recapitulated in Table 1. The crystal structure for all the compositions are indexed to the class of orthorhombic structure having space group (Pnma). It is observed that the substitution of K+ cation slightly increase the lattice parameter and unit cell volume. It might be due to larger ionic radii for K+ (1.38 Å) than Ba2+ (1.28Å) [18].

Compositions	$Pr_{0.7}Ba_{0.3}MnO_3$	$Pr_{0.7}Ba_{0.2}K_{0.1}MnO_3$
Lattice Parameters		
a(Å)	5.4408	5.4780
b(Å)	7.7002	7.7568
c(Å)	5.4777	5.4734
Lattice Volume		
V(Å)	229.86	232.57

We have calculated the lattice parameter using formula:

$$\frac{1}{d^2} = \frac{4}{3}\frac{(h^2+k^2+hk)}{a^2} + \frac{l^2}{c^2}$$

The calculated lattice parameter and lattice volume of $Pr_{0.7}Ba_{0.3-x}K_xMnO_3$ ($0 \leq x \leq 0.1$) are shown in above Table.

II. RESISTIVITY AND MAGNETO-RESISTANCE BEHAVIOR

The temperature dependence of electrical resistivity of the bulk samples $Pr_{0.7}Ba_{0.3-x}K_xMnO_3$ ($0 \leq x \leq 0.1$) in zero and applied field 8T is displayed in Fig.2 & 3. Within temperature range 2-300K. It is seen that the sample exhibit metal- insulator transition and the resistivity of sample gets suppressed under the applied magnetic fields. The resistance and the magneto-resistance (MR) behavior stem from the interplay of Jahn–Teller distortion, the strength of the Zener double exchange interaction, super-exchange and coulombic interactions, which can be controlled by the concentration of $Mn^{+3}(t^3_{2g}e^1_g)$ and $Mn^{4+}(t^3_{2g}e^0_g)$ valence states, which essentially changes the hole carrier density in the Mn–O–Mn sublattice. The decrease in resistivity at higher fields is due to the reason that interactions between the $Mn^{+3}(t^3_{2g}e^1_g)/Mn^{+4}(t^3_{2g}e^0_g)$ redox couple via the Oxygen atom in the Mn–O–Mn lattice.

The magneto resistance percentage (MR %) Vs temperature (T) plots of the above sample were investigated by a well known relation as:

$$MR\% = \frac{\rho 0 - \rho H}{\rho 0} \times 100$$

Where ρ_o and ρ_H are the resistivity in 0T and 8T magnetic fields respectively, It can be clearly seen from the Fig.3 that temperature dependent magneto resistance shows maximum MR% of 56% at a transition temperature T_c = 220. The magneto resistance is found to increase with rise in temperature and is maximum at 250K and thereafter decreases.

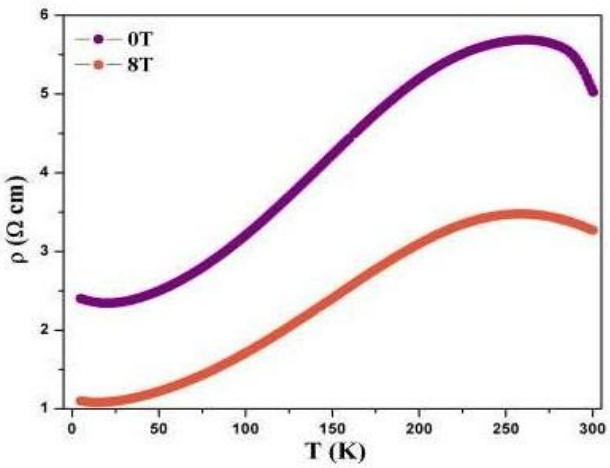

Figure: The temperature dependence of resistivity without and with magnetic field (8T) of Pr0.7Ba0.3MnO3.

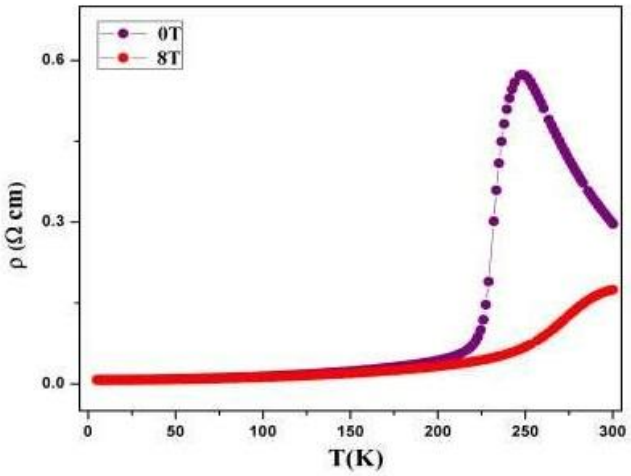

Figure: The temperature dependence of resistivity without and with magnetic field (8T) of $Pr_{0.7}Ba_{0.2}K_{0.1}MnO_3$.

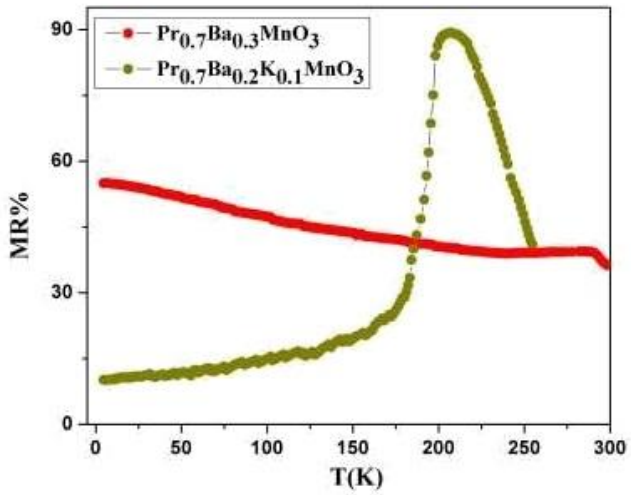

Figure: Temperature dependence magnetoresistance of $Pr_{0.7}Ba_{0.3-x}K_xMnO_3$ ($0 \leq x \leq 0.1$).

This indicates that K doping is beneficial to improve the intrinsic magneto-resistance of the material. The reason for increase in MR% might be the addition of K which can improve the defect of the grain surface, decrease the disorder degree of the particle surface and reduce the scattering function of itinerant electron with e_g and thus resulting in the decrease of resistivity at large scale.

REFERENCE

[1] Cavalcanti, Adriano; Bijan Shirinzadeh, Robert A Freitas Jr. and Tad Hogg, Nanotechnology, 19(2008).
[2] C.N.R. Rao "chemical Approach to the Synthesis of Inorganic materials' (JohnWile, New York 1994).
[3] Asbury, Charles L., Adrian N. Fehr and Steven M. Block, Science, 302(2003).
[4] I.J. Van der Paw Philips, Res. Repots, 16,187(1961)
[5] H.H. Weider "Laboratory notes on Electrical and Galvanornagnetic Measurement‟ Elsevier, Amsterdam 1979).
[6] A.A. Guzelian, J.E.B. Katari, A.V. Kadavanich, U. Banin And J.R. Health, J. Phys. Chem. 100, 7212(1996).
[7] Alivisatos, A.P., et al., Nature, 382 (1996).
[8] Y. Chen, G.Y.Jung, K.A.Nielsen, J.F. Stoddart, B. Gerardot, and R.S. Williams, Nanotechnology 14, 462 (2003).

